

Long-lived heavy neutral leptons at the LHC: four-fermion single- N_R operators

Rebeca Beltrán,^a Giovanna Cottin,^{b,c} Juan Carlos Helo,^{d,c} Martin Hirsch,^a Arsenii Titov,^e Zeren Simon Wang^{f,g}

^a*AHEP Group, Instituto de Física Corpuscular – CSIC/Universitat de València, Apartado 22085, E-46071 València, Spain*

^b*Departamento de Ciencias, Facultad de Artes Liberales, Universidad Adolfo Ibáñez, Diagonal Las Torres 2640, Santiago, Chile*

^c*Millennium Institute for Subatomic Physics at the High Energy Frontier (SAPHIR), Fernández Concha 700, Santiago, Chile*

^d*Departamento de Física, Facultad de Ciencias, Universidad de La Serena, Avenida Cisternas 1200, La Serena, Chile*

^e*Departament de Física Teòrica, Universitat de València and Instituto de Física Corpuscular – CSIC/Universitat de València, Dr. Moliner 50, E-46100 Burjassot, Spain*

^f*Department of Physics, National Tsing Hua University, Hsinchu 300, Taiwan*

^g*Center for Theory and Computation, National Tsing Hua University, Hsinchu 300, Taiwan*

E-mail: rebeca.beltran@ific.uv.es, giovanna.cottin@uai.cl, jchelo@userena.cl, mahirsch@ific.uv.es, arsenii.titov@ific.uv.es, wzs@mx.nthu.edu.tw

ABSTRACT: Interest in searches for heavy neutral leptons (HNLs) at the LHC has increased considerably in the past few years. In the minimal scenario, HNLs are produced and decay via their mixing with active neutrinos in the Standard Model (SM) spectrum. However, many SM extensions with HNLs have been discussed in the literature, which sometimes change expectations for LHC sensitivities drastically. In the N_R SMEFT, one extends the SM effective field theory with operators including SM singlet fermions, which allows to study HNL phenomenology in a “model independent” way. In this paper, we study the sensitivity of ATLAS to HNLs in the N_R SMEFT for four-fermion operators with a single HNL. These operators might dominate both production and decay of HNLs, and we find that new physics scales in excess of 20 TeV could be probed at the high-luminosity LHC.

Contents

1	Introduction	1
2	Effective theory with N_R	3
2.1	Effective interactions	3
2.2	Ultra-violet completions for four-fermion single- N_R operators	4
3	Simulation details	6
4	Numerical results	7
4.1	Minimal scenario	7
4.2	Four-fermion single- N_R operators	9
5	Summary	12

1 Introduction

Interest in long-lived particles (LLPs) has grown largely in the last few years [1–3]. Many models for LLPs have been discussed in the literature, most of which are motivated by either dark matter or neutrino masses. Heavy neutral leptons (HNLs) are the prime example for LLPs connected with the neutrino masses. HNLs are Standard Model (SM) singlet fermions that couple to SM particles via their mixing with active neutrinos.

The minimal model that can realize this effective setup is the seesaw mechanism, in which right-handed Majorana neutrinos, N_R , are added to the SM particle content [4–8]. However, many SM extensions, that aim to explain observed neutrino data [9] (see also Refs. [10, 11]) via electroweak scale variants of the classical seesaw [12–15], do not include only HNLs. For example, right-handed neutrinos appear necessarily in left-right (LR) symmetric extension of the SM as the neutral component of the right-lepton doublet [16, 17]. If the additional non-SM states, such as the W_R and Z' in the LR model, have masses which are too large to be produced on-shell at the LHC, their effects on HNL phenomenology is best treated in effective field theory (EFT).

The EFT of the SM, SMEFT, (see Ref. [18] for a review) is a well-established framework in LHC searches (for global analyses of collider data in this framework, see Refs. [19, 20]). The extension of the SMEFT to include right-handed neutrinos is called N_R SMEFT.¹ This EFT has been originally discussed in Refs [21, 22] and has attracted significant interest in the last few years, from both theoretical [23–29] and phenomenological [30–39] perspectives. Effective operators in the N_R SMEFT are now known up to dimension $d = 9$ [25].

¹In the literature, sometimes also called ν_R SMEFT.

Phenomenological interest in this EFT is motivated by the future upgrades of the LHC on one side and the improvement in the sensitivities of low-energy experiments on the other.

Effective interactions of $d \leq 6$ are the most interesting from a phenomenological point of view. There are two $d = 5$ operators involving N_R . Their phenomenology has been studied in detail in Refs. [22, 40, 41]. The $d = 6$ operators containing N_R can be divided into two classes: (i) operators with two fermions and bosons and (ii) four-fermion operators. The second class, in turn, can be partitioned into operators with two N_R 's and operators with a single N_R .² The LLP phenomenology of pair operators has recently been studied in Ref. [39]. Here, we will concentrate on operators with a single N_R . The phenomenology of single- N_R operators is decidedly different from that of pair operators. First, pair operators do not by themselves lead to decays of (the lightest) N_R . Instead, for these operators N_R decays are controlled by the mixing with active neutrinos. This is different from the single- N_R operators, which will usually dominate the decay length of the HNLs in those parts of parameter space where the operators are large enough to dominate N_R production. Thus, the parameter space that can be explored for these two types of operators is very different, see Sec. 4. Second, pair operators do not produce prompt charged leptons, except in the parameter region where the decay length of the N_R is so short that the lepton from a N_R decay is confused with a charged lepton produced directly from pp collisions at the interaction point (IP). In all lepton-number-conserving single- N_R operators, on the other hand, N_R 's are accompanied by a prompt lepton (either a neutrino or a charged lepton). This affects the search strategy for the different operators.

Ref. [38] studied single- N_R operators for various proposed LLP “far” detectors, such as MATHUSLA [3, 42, 43], CODEXb [44], AL3X [45], FASER [46], and ANUBIS [47], as well as ATLAS, for HNLs produced from charm and bottom meson decays and hence with mass below 5 GeV.³ In addition, Ref. [51] very recently worked on phenomenology of the same set of single- N_R operators associated with the third-generation leptons at Belle II, for HNLs produced from τ lepton decays. For these reasons, in our numerical simulation we concentrate on ATLAS for heavier HNLs, and a short discussion will also be given for the expectations for CMS (see Sec. 4).

The rest of this paper is organized as follows. In the next section, we will discuss briefly N_R SMEFT at $d = 6$. This section also entails a short discussion on how the single- N_R operators could be the low-energy remnant of some leptoquark or two Higgs doublet models. Sec. 3 discusses the details of the simulation we perform for the ATLAS detector. In Sec. 4, we present our numerical results. First, we discuss again briefly the minimal case, in which HNLs are produced and decay via mixing only. While this was previously done by some of us in Ref. [52], we now also simulate the expectations for HNLs coupled to τ 's, including both neutral and charged currents leading to more realistic estimates for

²There is also a lepton-number-violating operator with four N_R 's, but it requires at least two generations of HNLs.

³For the expectations for these experiments in the minimal HNL scenario with only active-sterile neutrino mixing, see for example Refs. [48–50].

the future ATLAS sensitivities. We then present our results for the different single- N_R operators. Cross sections and decay lengths depend on both, operator type and generation indices in the SM sector. For the first generation of SM quarks, sensitivities will reach new physics scales in excess of 20 TeV at the high-luminosity LHC. We then close with a short summary of our results.

2 Effective theory with N_R

2.1 Effective interactions

In this section, we briefly introduce the N_R SMEFT, focusing on the operators of interest for the current work. If HNLs with masses below or around the electroweak scale exist in nature, the effects of new multi-TeV physics at much smaller energies can be systematically described in terms of an EFT built out of the SM fields and N_R . At renormalizable level, in addition to the SM operators, there are a Majorana mass term for N_R and a $d = 4$ operator describing the fermion portal:

$$\mathcal{L}_{\text{ren}} = \mathcal{L}_{\text{SM}} + \overline{N_R} i \not{\partial} N_R - \left[\frac{1}{2} \overline{N_R^c} M_N N_R + \overline{L} \tilde{H} Y_N N_R + \text{h.c.} \right], \quad (2.1)$$

where L stands for the SM lepton doublets, H is the Higgs doublet ($\tilde{H} = \epsilon H^*$, ϵ is the totally antisymmetric tensor), and $N_R^c \equiv C \overline{N_R}^T$ with C being the Dirac charge conjugation matrix. The Majorana mass matrix M_N is a symmetric $n_N \times n_N$ matrix, with n_N denoting the number of HNL generations, and Y_N is a generic $3 \times n_N$ matrix of Yukawa couplings.

Upon including non-renormalizable interactions $\mathcal{O}_i^{(d)}$ with $d \geq 5$, the full Lagrangian reads

$$\mathcal{L} = \mathcal{L}_{\text{ren}} + \sum_{d \geq 5} \frac{1}{\Lambda^{d-4}} \sum_i c_i^{(d)} \mathcal{O}_i^{(d)}, \quad (2.2)$$

where $c_i^{(d)}$ are the Wilson coefficients, and the second sum goes over all independent interactions at a given dimension d . At $d = 5$, in addition to the renowned Weinberg operator composed of L and H [53], one finds two more operators that involve N_R [21, 22].

At $d = 6$, in addition to the pure SMEFT operators [54], there are five operators involving two fermions (at least one of which is N_R) and bosons, eleven baryon and lepton-number-conserving four-fermion interactions, one lepton-number-violating operator, and two operators that violate both baryon and lepton number [24].⁴ In the present work, we are interested in the effects of the lepton-number-conserving four-fermion interactions containing one N_R and three SM fermions. We list them in Table 1. The effects of the four-fermion operators containing a pair of HNLs and a pair of quarks have been investigated in detail in Ref. [39].

The single- N_R operators including quarks can lead to enhanced HNL production cross section at the LHC, but they also trigger the decay of N_R to a lepton and two quarks.

⁴Here, we count the operator types, *i.e.* we do not take into account the flavor structure and do not count hermitian conjugates.

Name	Structure (+ h.c.)	$n_N = 1$	$n_N = 3$
\mathcal{O}_{duNe}	$(\bar{d}_R \gamma^\mu u_R) (\bar{N}_R \gamma_\mu e_R)$	54	162
\mathcal{O}_{LNQd}	$(\bar{L} N_R) \epsilon (\bar{Q} d_R)$	54	162
\mathcal{O}_{LdQN}	$(\bar{L} d_R) \epsilon (\bar{Q} N_R)$	54	162
\mathcal{O}_{QuNL}	$(\bar{Q} u_R) (\bar{N}_R L)$	54	162
\mathcal{O}_{LNLe}	$(\bar{L} N_R) \epsilon (\bar{L} e_R)$	54	162

Table 1. Lepton-number-conserving four-fermion single- N_R operators. For each operator structure, we provide the number of independent real parameters for $n_N = 1$ and $n_N = 3$ generations of N_R . The operator in the last row is purely leptonic, and thus, it does not contribute to the HNL production at the LHC.

The total decay width of the N_R 's depends on the operator. Neglecting the masses of the lepton and light quarks, the partial decay width to charged leptons plus quarks is given by

$$\Gamma(N_R \rightarrow \ell q q') = \frac{c_{\mathcal{O}}^2 m_N^5}{f_{\mathcal{O}} 512 \pi^3 \Lambda^4}, \quad (2.3)$$

with m_N being the HNL mass, $c_{\mathcal{O}}$ the Wilson coefficient of the operator \mathcal{O} , and $f_{\mathcal{O}}$ the numerical factor depending on the operator type. For \mathcal{O}_{duNe} $f_{\mathcal{O}} = 1$, whereas for \mathcal{O}_{LNQd} , \mathcal{O}_{LdQN} , and \mathcal{O}_{QuNL} $f_{\mathcal{O}} = 4$. To arrive at the total decay width, one has to add also the final state with neutrinos for all operators, except \mathcal{O}_{duNe} . Since the partial width to neutrinos follows the same equation as for charged leptons, this results in total decay widths being twice the partial decay widths given in Eq. (2.3) (again, except for \mathcal{O}_{duNe}). Finally, Eq. (2.3) applies to Dirac neutrinos. For Majorana neutrinos, one has to add also the charged conjugated channels, leading to another factor of 2 for the widths.

2.2 Ultra-violet completions for four-fermion single- N_R operators

The single- N_R operators of interest can be generated in ultra-violet (UV) complete models containing heavy scalars or vectors. Here, we do not aim to provide a complete classification of such UV completions, but rather give a few examples. In what follows, we consider scalar leptoquarks and an inert $SU(2)_L$ doublet scalar. A catalog of models with scalar and vector leptoquarks generating four-fermion operators involving one or two N_R 's and quarks can be found in Ref. [30].

The operator \mathcal{O}_{duNe} can arise from a model with a scalar leptoquark S_d having the gauge quantum numbers of the down quark, cf. Table 2. The interaction Lagrangian of S_d is given by

$$-\mathcal{L}_{S_d} = g_{dN} \bar{d}_R N_R^c S_d + g_{ue} \bar{u}_R e_R^c S_d + g_{QL} \bar{Q} \epsilon L^c S_d + \text{h.c.} \quad (2.4)$$

Upon integrating out S_d , the operator \mathcal{O}_{duNe} is generated with the tree-level matching condition for the Wilson coefficient c_{duNe} given in the last column of Table 2.⁵ Analogously,

⁵For simplicity, here, we assume the renormalizable couplings to be real and suppress flavor indices. The factor of two in the denominator originates from a Fierz identity.

Heavy scalar	$SU(3)_C$	$SU(2)_L$	$U(1)_Y$	Operator	Matching relation
Leptoquark S_d	3	1	$-1/3$	\mathcal{O}_{duNe}	$\frac{c_{duNe}}{\Lambda^2} = \frac{g_{dN}g_{ue}}{2m_{S_d}^2}$
Leptoquark S_Q	3	2	$1/6$	\mathcal{O}_{LdQN}	$\frac{c_{LdQN}}{\Lambda^2} = \frac{g_{dL}g_{QN}}{m_{S_Q}^2}$
Inert doublet Φ	1	2	$1/2$	\mathcal{O}_{LNQd}	$\frac{c_{LNQd}}{\Lambda^2} = \frac{g_{LN}g_{Qd}}{m_{\Phi}^2}$
				\mathcal{O}_{QuNL}	$\frac{c_{QuNL}}{\Lambda^2} = \frac{g_{Qu}g_{LN}}{m_{\Phi}^2}$

Table 2. Heavy scalars with their gauge quantum numbers and the four-fermion single- N_R operators they can generate. The last column reports the tree-level matching relations between the Wilson coefficients and the couplings of the UV model.

a scalar leptoquark S_Q with the quantum numbers of the $SU(2)_L$ quark doublet can lead to \mathcal{O}_{LdQN} . The Yukawa interactions of S_Q read

$$-\mathcal{L}_{S_Q} = g_{QN}\bar{Q}N_R S_Q + g_{dL}\bar{d}_R L^T \epsilon S_Q + \text{h.c.} \quad (2.5)$$

We note that the first terms in Eqs. (2.4) and (2.5) also generate the N_R pair operators $\mathcal{O}_{qN} = (\bar{q}\gamma^\mu q)(\bar{N}_R\gamma_\mu N_R)$, where $q = d_R$ and $q = Q$, respectively, cf. Ref. [39].

The operators \mathcal{O}_{LNQd} and \mathcal{O}_{QuNL} , in turn, can originate from a two Higgs doublet model, after the second, heavy doublet Φ has been integrated out. The interactions of interest in the UV model have the following form:

$$-\mathcal{L}_{\Phi} = g_{Qd}\bar{Q}\Phi d_R + g_{Qu}\bar{Q}\tilde{\Phi}u_R + g_{LN}\bar{L}\tilde{\Phi}N_R + \text{h.c.}, \quad (2.6)$$

where $\tilde{\Phi} = \epsilon\Phi^*$. From Table 2, it is clear that the Wilson coefficients of the operators depend on different combinations of independent couplings in the UV model. Therefore, in this example, the generated operators are uncorrelated.

We have implemented these renormalizable models in `FeynRules` [55, 56] for both Dirac and Majorana N_R . Using the generated UFO [57] model files and `MadGraph5` [58, 59], we have checked that both cases lead to the same single- N_R production cross section. We note that for N_R pair production triggered by the four-fermion operators with two N_R 's, the cross section is different for Dirac and Majorana HNLs, especially for values of $m_N \gtrsim 100$ GeV at LHC energies (we refer the interested reader to Sec. 3.1 of Ref. [39]). The fact that the HNL nature does not affect the production triggered by the four-fermion single- N_R operators allows us to implement these operators directly in `FeynRules` for Dirac HNLs and use the resulting UFO model file in `MadGraph5`. (Recall that `MadGraph5` can not handle Majorana fermions in operators with more than two fermions, cf. Sec. 3.1 of Ref. [39].)

3 Simulation details

Our signal topology contains a prompt lepton and a displaced vertex (DV) stemming from the N_R decay to leptons and quarks. Our stage to reconstruct such a signature is the ATLAS detector, specifically its inner tracker, as it has the capability to reconstruct vertices displaced from the IP by few millimeters to tens of centimeters. Our analysis strategy builds up on an earlier work [52] and is inspired from ATLAS multi-track displaced searches [60, 61].

We consider the collision process $pp \rightarrow Nl$ with $l = e, \mu, \tau$, at $\sqrt{s} = 14$ TeV at the high-luminosity LHC with an integrated luminosity of 3 ab^{-1} . We generate LHE events with displaced information at the parton level with `MadGraph5`, which are read by `Pythia8` [62] for showering and hadronization. Our detector simulation is based on a custom made code within `Pythia8`, where we first reconstruct isolated prompt electrons, muons, and taus (with help from `FastJet` [63]), taking into account detector acceptance, resolution, and smearing on their transverse momenta (for details, see Ref. [52]). After selecting events with a prompt lepton, the displaced vertex reconstruction starts by selecting tracks⁶ with $p_T > 1$ GeV and a large impact parameter, d_0 , defined as $d_0 = r_{\text{trk}} \times \Delta\phi$. Here $\Delta\phi$ corresponds to the azimuthal angle between the track and the direction of the long-lived N_R , and r_{trk} corresponds to the transverse distance of the track from the origin. We require $|d_0| > 2$ mm.

As we have access in simulation to truth-level Monte Carlo information, we also identify the truth N_R decay positions in the transverse and longitudinal planes, namely, r_{DV} and z_{DV} , respectively. An additional step (with respect to Ref. [52]) of the vertex reconstruction implemented in this work is the requirement that $r_{\text{trk}} - r_{\text{DV}} < 4$ mm. It is not always the case that the “starting” point of the displaced track matches the displaced vertex position. This is more evident in the case where we have a tau produced from the N_R displaced decay, as taus also have an additional displacement.⁷ With this requirement, we emulate what an experimental displaced-vertex reconstruction would do when fitting nearby displaced tracks to a common origin [60]. This will lead to an additional reduction in efficiency when reconstructing displaced vertices containing taus. Nevertheless, it is a more realistic (and optimistic) approach than what was done in Ref. [52] to handle heavy neutrino decays to taus (see Sec. 4 below).

After selecting optimal displaced tracks, we demand displaced vertices within the ATLAS inner tracker acceptance, namely, $4 \text{ mm} < r_{\text{DV}} < 300 \text{ mm}$ and $|z_{\text{DV}}| < 300 \text{ mm}$. Further cuts are applied on the number of high-quality tracks coming from the DV, N_{trk} , and its invariant mass, m_{DV} , assuming all tracks have the pion mass. More concretely, we require $N_{\text{trk}} > 3$ and $m_{\text{DV}} \geq 5$ GeV. As detailed in Refs. [60, 61, 64], these last two cuts

⁶A track in our simulation is a final state charged particle. These come from the decays of N_R and can correspond to an electron, a muon, or a charged particle coming from the hadronization of quarks or from tau decays.

⁷The proper decay distance of tau leptons is $c\tau = 87.1 \text{ }\mu\text{m}$. This will lead, for example, to decay distances of $\gamma c\tau \sim 5 \text{ mm}$ at 100 GeV.

ensure that we are in a region where signal is expected to be found free of backgrounds including B -mesons. Further detector response to DVs is quantified by applying the 13 TeV ATLAS parameterized efficiencies [61] as a function of DV invariant mass and number of tracks, where we assume these will remain the same at 14 TeV.

4 Numerical results

Based on the computational procedure described in the previous section, we have estimated the experimental sensitivities (95 % confidence level (C.L.) exclusion limits under the assumption of zero background) of searches for long-lived HNLs at the ATLAS detector for two different theoretical scenarios. The first is the minimal scenario in which only right-handed neutrinos, N_R , are added to the particle content of the SM and renormalizable interactions are assumed. In this case, the HNLs interact with the SM particles only through the mixing with the active neutrinos, V_{lN} , with $l = e, \mu, \tau$. In the second theoretical scenario we consider N_R SMEFT containing non-renormalizable interactions of N_R with the SM. In this case, both production and decay of the HNLs can be mediated by the single- N_R effective operators under consideration. In all of the plots below, we assume a $3 + 1$ scenario where the HNL mixes dominantly with only one active neutrino flavor at a time. We assume only one HNL is kinematically relevant.

4.1 Minimal scenario

In the minimal scenario, the relevant parameters are the mass of the HNL, m_N , and the mixing of the HNL with the active neutrinos, V_{lN} , which we have treated as independent parameters. The HNLs are produced from the decays of on-shell W -bosons into a lepton and an HNL associated with a charged lepton, $pp \rightarrow W \rightarrow lN$, via the HNL mixing with the active neutrinos. The decay of the HNLs occurs also via the mixing with the active neutrinos, through both charged and neutral SM currents, $N \rightarrow l(\nu)jj$. For the minimal scenario we use the `FeynRules` implementation for HNLs of Ref. [65].

Figure 1 shows the region, in the plane $|V_{lN}|^2$ vs. m_N , where a displaced-vertex search at the ATLAS detector for the center-of-mass energy 14 TeV, and with the selection criteria discussed in Sec. 3, may have sensitivity to the minimal scenario. As can be seen in this figure, the sensitivities in $|V_{eN}|^2$ and $|V_{\mu N}|^2$ are rather similar and can reach values down to $|V_{lN}|^2 \sim 10^{-9}$ for $m_N \sim 30$ GeV, with 3 ab^{-1} of integrated luminosity. On the other hand, in the case of mixing with the tau neutrinos, ATLAS can reach values of the mixing parameter down to $|V_{\tau N}|^2 \sim 5 \times 10^{-9}$ for $m_N \sim 20$ GeV with 3 ab^{-1} . Figure 1 compares our limits with the current experimental bounds for this model, represented by the dark gray area at the top of each plot. These constraints were obtained at the following experiments: ATLAS [66], CMS [67, 68], DELPHI [69], and LHCb [70, 71]. As we can see, our forecast limits can reach values of the mixing $|V_{lN}|^2$ several orders of magnitude smaller than current experimental bounds.

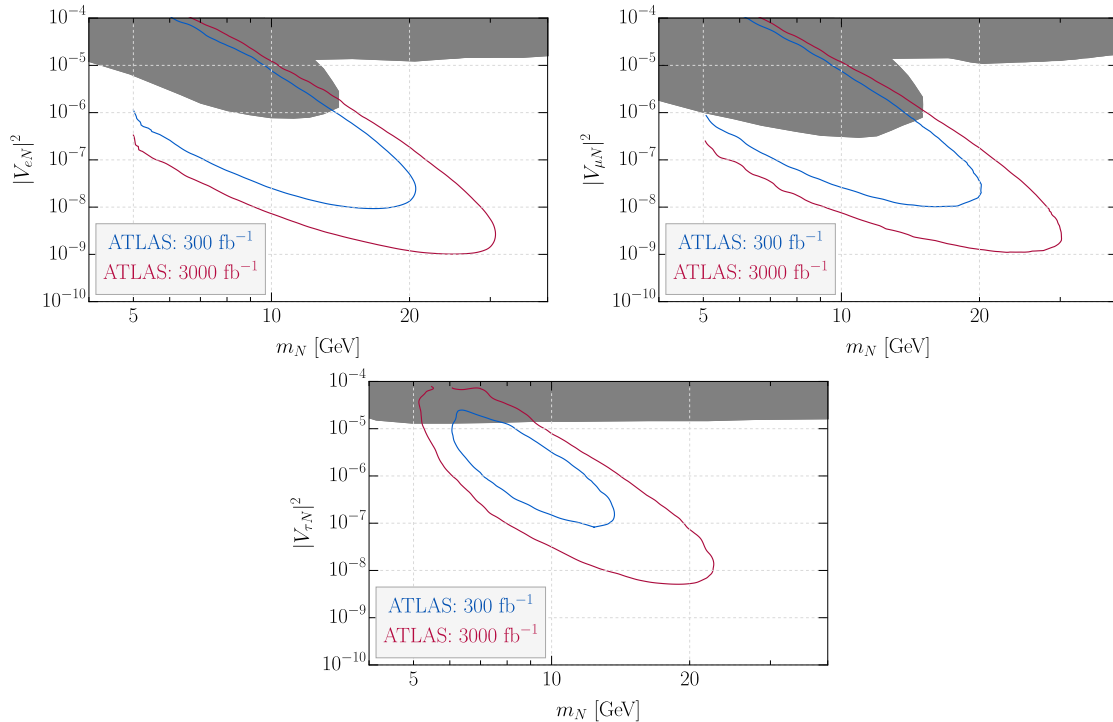


Figure 1. Minimal scenario sensitivity reach on $|V_{lN}|^2$ as a function of m_N , for $l = e, \mu, \tau$. The dark region corresponds to current experimental limits obtained at several experiments: ATLAS [66], CMS [67, 68], DELPHI [69], and LHCb [70, 71].

It might be interesting to compare the forecast limits to theory expectations. In seesaw type-I, one naively expects $|V_{lN}|^2 \simeq m_\nu/m_N \simeq (10^{-12} - 10^{-11})$ for values of m_N in the range we are considering in this work. Larger values of $|V_{lN}|^2$ are possible allowing fine-tuning in parameters. A more natural model for having $|V_{lN}|^2$ in the range accessible for ATLAS/CMS might be the inverse seesaw [12]. In this variant of the seesaw, $|V_{lN}|^2$ is given by $|V_{lN}|^2 \simeq m_\nu/\mu$, with μ being the lepton-number-violating parameter of the inverse seesaw model. With μ supposedly being a small parameter, when compared to m_N , mixings in this model can be easily as large as the experimental limits.

As mentioned above, the same search strategy for long-lived HNLs was previously proposed by some of us in Ref. [52]. One of the differences between our current and previous calculations is the center-of-mass energy at the LHC, which now is taken as 14 TeV (previously in Ref. [52] we used 13 TeV). Perhaps more important is the fact that in the present paper, our numerical calculations used more statistics, which allowed us to obtain much smoother contours for our limits, which led to a slight increase in the ranges shown. Moreover, in the case of mixing with taus, our current limits are more sensitive than the previous ones calculated in Ref. [52]. The reason for this difference is that in Ref. [52], we only considered neutral currents in the decay of HNLs that coupled to taus (i.e. we ignored a tau lepton coming from the displaced vertex), whereas now, we have included both charged and neutral currents in our calculations, making our limits more realistic for

the case of the mixing with the tau neutrinos and comparable with the sensitivity reach projected with other proposed strategies (see for instance Ref. [72]).

4.2 Four-fermion single- N_R operators

In the second theoretical scenario, we consider the four-fermion single- N_R operators in the N_R SMEFT. We estimate the experimental sensitivity of our displaced search to a long-lived HNL at the ATLAS detector. Here, we take the coefficients of the operators $c_{\mathcal{O}}/\Lambda^2$ and the mass of the HNL, m_N , as independent parameters. In this scenario, both the production and the decay of the HNL can be dominated by the same operator \mathcal{O} , unlike the case of effective operators with two HNLs [39], where the pair- N_R operators dominantly induce the HNL production, but the decay of the HNL still proceeds only via mixing with the active neutrinos. For the EFT scenario, in our analysis we have assumed that the contributions to the production and decay of the HNL from its mixing with active neutrinos V_{lN} are subdominant and negligible compared to the effective operators' contributions. For mixing angles smaller than $|V_{lN}|^2 \lesssim 10^{-9}$, this assumption is always fulfilled.

The production of the HNLs considered in our analysis, $pp \rightarrow lN$, is always accompanied by a prompt charged lepton — an electron, muon, or tau, depending on the flavor structure of the effective operator considered. The presence of this charged lepton is important in our analysis as it is used to trigger the signal, as discussed in Sec. 3. The decay of the HNLs will occur via the same operator leading to two jets and one neutral or charged lepton, $N \rightarrow l(\nu)jj$. The production cross sections of the HNLs will depend on the type of quarks that the respective operator includes. In our analysis, we have only considered effective operators with quarks of the first two generations.

In Fig. 2, we show the experimental sensitivity of the ATLAS detector to a long-lived HNL in the Λ vs. m_N plane. In our analysis, we have considered the contributions of one operator at a time, setting the value of the corresponding operator coefficient $c_{\mathcal{O}} = 1$, and the rest of the operator coefficients to zero. In Fig. 2, we have considered only operators with quarks of the first generation. Note that the numbers in the superscript of *e.g.* c_{duNe}^{1112} refer to the first-generation quarks (d and u), the lightest N_R and the second-generation charged lepton (the muon). As can be seen in this figure, for an integrated luminosity of 3 ab^{-1} , ATLAS can reach values of the new physics scale up to (and above) $\Lambda \sim 20 \text{ TeV}$ for masses $m_N \lesssim 50 \text{ GeV}$ in the case of operators with an electron or muon. In the case of operators with a tau lepton, ATLAS can reach $\Lambda \gtrsim 10 \text{ TeV}$ at masses m_N of 10's GeV. It is worth mentioning that our limits start at $m_N \gtrsim 5 \text{ GeV}$. The reason is the kinematic cut at $m_{DV} \geq 5 \text{ GeV}$ imposed in the selection criteria. This cut is necessary to remove the SM background coming from B -mesons, as discussed in Sec. 3. We also note that the projected exclusion limits are rather similar for the four types of single- N_R operators, in particular for \mathcal{O}_{LNQd} and \mathcal{O}_{QuNL} .

Figure 3 contains our limits in the plane Λ vs. m_N for the effective operators with quarks of the second generation only. As expected, the sensitivity regions for operators with quarks of the second generation only are smaller than those corresponding to operators

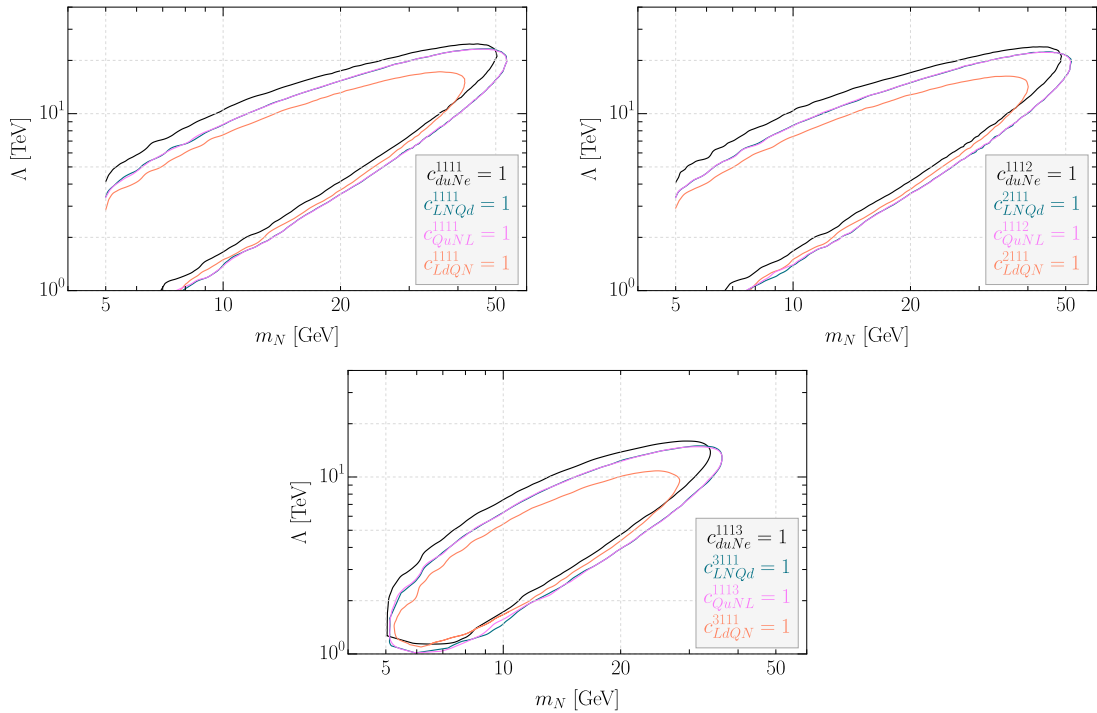


Figure 2. Exclusion limits on the new physics scale Λ as a function of m_N in the EFT scenario with operators including the first-generation quarks only, for an integrated luminosity of 3 ab^{-1} . The two plots at the top consider operators with charged leptons of the first and second generation: electrons (left) and muons (right). The plot at the bottom considers operators with tau leptons only.

with first-generation quarks (Fig. 2). This is due to the predominant content of quarks u and d in the proton versus the quarks c and s . We find that limits shown in Fig. 3 can reach $\Lambda \sim 13 \text{ TeV}$ for $m_N \sim 23 \text{ GeV}$ in the cases of electrons and muons, and up to $\Lambda \sim 9 \text{ TeV}$ for $m_N \sim 18 \text{ GeV}$ in the case of taus. All numbers assume an integrated luminosity of 3 ab^{-1} . Other possible combinations of quark flavors for the N_R SMEFT include (u, s) and (c, d) . The sensitivity reaches for these operators lie between the two cases shown in Figs. 2 and 3 (for (u, d) and (c, s)). We therefore do not show results for these cases explicitly. Operators with third-generation quarks have not been considered in this work, since they will require special treatment (i.e. tagging).

We also note that Figs. 2 and 3 have been calculated for Dirac HNLs. As mentioned above, production cross sections for single- N_R operators are the same for Dirac and Majorana HNLs, while the half-lives for Majorana HNLs are smaller by a factor of two. The sensitivity regions for Majorana HNLs therefore differ slightly from the regions shown in the figures. We do not repeat the plots for the Majorana case and instead opt for a short explanation of the differences. First, the maximal value of the HNL mass, to which this kind of search is sensitive is determined by the smallest decay length that is accessible in the experiment. Since the decay width scales as m_N^5 , for a Majorana HNL the largest HNL

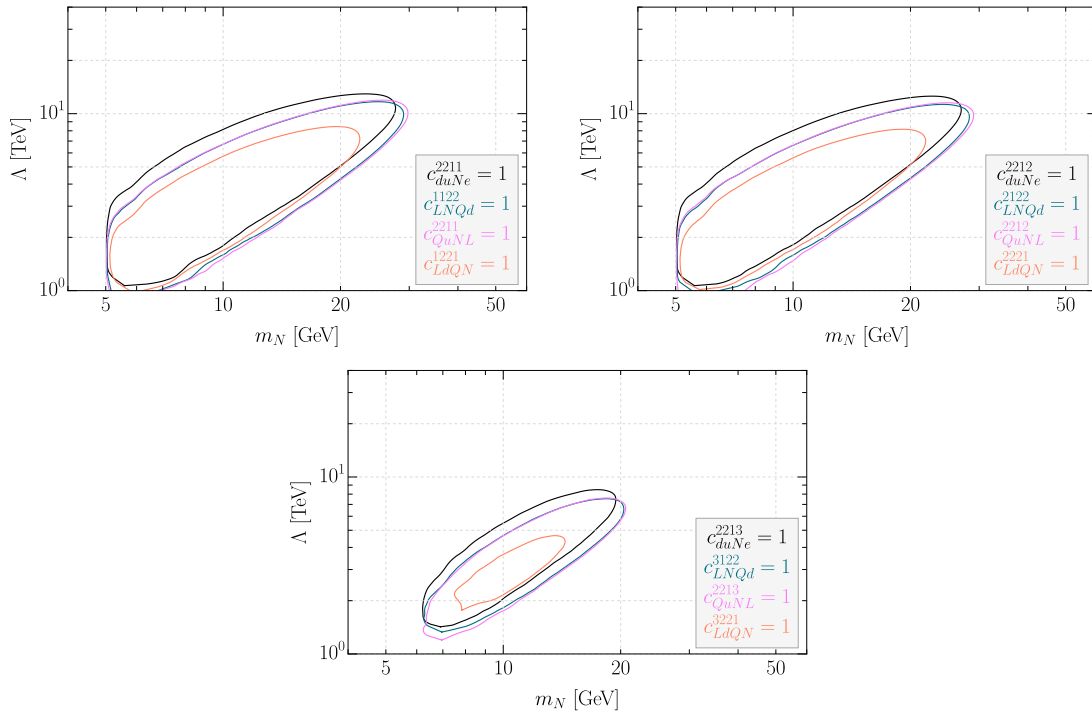


Figure 3. The same as Fig. 2, but for operators with second-generation quarks only.

mass accessible is a factor $(1/2)^{1/5} \simeq 0.87$ smaller than in the Dirac case. Second, the maximal value of Λ reached in our sensitivity curves is essentially determined by the total cross section (times luminosity). Since cross sections are the same for Dirac and Majorana HNLs, this maximal value of Λ does not change for Majorana HNLs. Finally, in the regime where the decay lengths are large (i.e. for large values of Λ at values of m_N smaller than the one where the maximal value of Λ is reached), the event number depends linearly on the half-life, while both the cross section and the decay width scale as Λ^{-4} . For Majorana HNLs, in this part of the parameter space, slightly larger values of Λ are accessible than for the Dirac case, i.e. an increase by roughly a factor $2^{1/8} \simeq 1.09$.

Let us briefly comment on existing limits. First of all, our choice of switching “on” always only one Wilson coefficient at a time guarantees that there is no new source of lepton (or quark) flavour violation. It is well known that ultra-violet completions, such as the leptoquark models we discuss in Sec. 2.2, are strongly constrained by searches for lepton-flavor-violating processes. These will put lower bounds on $m_{LQ} \simeq \Lambda$ that are much stronger than anything achievable in direct searches [73, 74]. Thus, *in all accelerator searches* it is customary to assume that new resonances, such as leptoquarks, couple only to one SM fermion generation at a time. Direct searches for leptoquarks from pair and single leptoquark production have been performed by both, CMS [75–77] and ATLAS [78, 79]. The best limits approach now $m_{LQ} \simeq 2$ TeV. Thus, the long-lived particle search discussed in this paper, will probe so-far uncharted parts of parameter space. Let us also mention,

that since $d = 6$ operators have Wilson coefficients of the form c/Λ^2 , limits on Λ will scale proportional to \sqrt{c} . Thus for $c \lesssim 10^{-2}$ our search will no longer probe values of Λ not already excluded by direct LHC searches.

We will close this discussion with one additional comment. Our simulated analysis focused on the ATLAS detector and its reconstruction capabilities to displaced vertices inside the inner tracker, starting from 4 mm in multi-track searches [60, 61]. Relaxing this requirement to decay distances below 4 mm (both in d_0 , r_{DV} and z_{DV}) will allow to extend the reach in parameter space towards larger HNL masses. Of course, with the loosening of these cuts we may depart from the zero background case assumption, and a detailed study on the multi-track search backgrounds would be needed, which goes beyond the scope of the present work. Nevertheless, past displaced lepton searches – whose tracks are fitted to a common vertex – at CMS [80] could probe transverse decay lengths starting from $\approx 200 \mu\text{m}$ ⁸. In addition, a recent 13 TeV CMS search [81] demonstrates that lepton tracks with $|d_0| > 0.1$ mm are displaced enough to be considered for analysis. Finally, the recent CMS note on an HNL search with an explicit displaced vertex requirement does not even demand a constraint on the DV minimal distance [68]. This provides feasibility to experimentally go below the 4 mm threshold. We stress that an improvement of the displaced vertex search towards smaller decay lengths by such a larger factor (up to 40 for 0.1mm) would allow to test HNL masses larger by a factor 2 w.r.t the values in our figures, i.e. extend the searches from $m_N \simeq 50$ GeV to roughly 100 GeV. We hope that this large potential gain motivates the experimental collaborations to study the lowering of the transverse cuts in displaced vertex searches to the sub-millimeter range.

5 Summary

The Standard Model (SM) effective field theory (EFT) extended with sterile neutrinos, also known as the N_R SMEFT, provides a framework to systematically study sterile neutrinos associated with a high new-physics (NP) scale in ultra-violet complete models beyond the SM. In the N_R SMEFT, high-scale NP effects are encoded in the so-called Wilson coefficients of non-renormalizable operators at different mass dimensions. Higher-dimensional operators involving N_R can have either one, two, or four sterile neutrinos, and may conserve or violate lepton number, or else both lepton and baryon numbers.

In this work, we have focused on lepton-number-conserving four-fermion single- N_R operators associated with a charged lepton and two quarks, which can induce both production and decay of the heavy neutral leptons (HNLs) simultaneously. For HNLs of $\mathcal{O}(10)$ GeV mass, such operators with a NP scale above ~ 1 TeV can easily make the HNLs become long-lived, leading to displaced vertices at the LHC. We have therefore proposed a displaced-vertex search strategy based on a prompt-lepton trigger and selection of high-quality displaced tracks. By performing Monte-Carlo simulations with `MadGraph5` and

⁸The explicit analysis requirement in Ref. [80] demands tracks to have a transverse impact parameter significance with respect to the primary vertex of $|d_0|/\sigma_d > 12$, where σ_d is the uncertainty on $|d_0|$.

Pythia8, we have estimated the sensitivity reaches for ATLAS in the high-luminosity LHC era with 3 ab^{-1} integrated luminosity, to four single- N_R EFT operators: \mathcal{O}_{duNe} , \mathcal{O}_{LNQd} , \mathcal{O}_{LdQN} , and \mathcal{O}_{QuNL} .

Multiple combinations of quark and lepton flavors can be studied. Here, we have considered mainly two combinations: (u, d) and (c, s) . The first (second)-generation-quark only flavor combination is then projected to have the best (worst) sensitivities, because of their portion in the proton content. For both quark combinations, we also studied all possible lepton generations, i.e. electron, muon and tau. In addition, for simplicity, we did not take into account the effect of the active-sterile neutrino mixing, which is supposed to be negligible if the type-I seesaw relation is assumed. For the (u, d) and (c, s) combinations, we find in general for the considered single- N_R operators, ATLAS can probe Λ up to 20 TeV and above for $m_N \gtrsim 20$ GeV, if we switch on one operator at a time.

In addition to the EFT scenarios, we also revisited the minimal scenario of the HNL mixing with the SM neutrinos. In this scenario, the type-I seesaw relation is not assumed and we have two independent parameters: mass of the HNL and its mixing parameter with one type of the active neutrinos: a simple $3 + 1$ scenario. These results are an update of those given in Ref. [52]. Besides some minor changes, the most important difference is that we have now taken into account both charged and neutral currents in our computation, leading to more realistic projection results, especially for the case of mixing with the τ neutrino.

In summary, we conclude that a displaced-vertex search at ATLAS for HNLs can probe new physics scales up to about 20 TeV and, in some cases above, for HNL mass between about 5 GeV and 50 GeV, depending on the quark and lepton flavors associated with the single- N_R operator under consideration.

Acknowledgements

This work is supported by the Spanish grants PID2020-113775GB-I00 (AEI/10.13039/501100011033) and PROMETEO/2018/165 (Generalitat Valenciana). R.B. acknowledges financial support from the Generalitat Valenciana (grant ACIF/2021/052) and CSIC (JAE ICU-20-IFIC-2). G.C. acknowledges support from ANID FONDECYT-Chile grant No. 3190051. G.C. and J.C.H. also acknowledge support from grant ANID FONDECYT-Chile No. 1201673 and ANID – Millennium Science Initiative Program ICN2019_044. The work of A.T. is supported by the “Generalitat Valenciana” under grant PROMETEO/2019/087, as well as by the FEDER/MCIyU-AEI grant FPA2017-84543-P and the AEI-MICINN grant PID2020-113334GB-I00 (AEI/10.13039/501100011033). Z.S.W. is supported by the Ministry of Science and Technology (MoST) of Taiwan with grant numbers MoST-109-2811-M-007-509 and MoST-110-2811-M-007-542-MY3.

References

- [1] J. Alimena et al., *Searching for long-lived particles beyond the Standard Model at the Large Hadron Collider*, *J. Phys. G* **47** (2020) 090501 [[1903.04497](#)].
- [2] L. Lee, C. Ohm, A. Soffer and T.-T. Yu, *Collider Searches for Long-Lived Particles Beyond the Standard Model*, *Prog. Part. Nucl. Phys.* **106** (2019) 210 [[1810.12602](#)].
- [3] D. Curtin et al., *Long-Lived Particles at the Energy Frontier: The MATHUSLA Physics Case*, *Rept. Prog. Phys.* **82** (2019) 116201 [[1806.07396](#)].
- [4] P. Minkowski, $\mu \rightarrow e\gamma$ at a Rate of One Out of 10^9 Muon Decays?, *Phys. Lett. B* **67** (1977) 421.
- [5] T. Yanagida, *Horizontal gauge symmetry and masses of neutrinos*, *Conf. Proc. C* **7902131** (1979) 95.
- [6] M. Gell-Mann, P. Ramond and R. Slansky, *Complex Spinors and Unified Theories*, *Conf. Proc. C* **790927** (1979) 315 [[1306.4669](#)].
- [7] R.N. Mohapatra and G. Senjanovic, *Neutrino Mass and Spontaneous Parity Nonconservation*, *Phys. Rev. Lett.* **44** (1980) 912.
- [8] J. Schechter and J.W.F. Valle, *Neutrino Masses in $SU(2) \times U(1)$ Theories*, *Phys. Rev. D* **22** (1980) 2227.
- [9] P.F. de Salas, D.V. Forero, S. Gariazzo, P. Martínez-Miravé, O. Mena, C.A. Ternes et al., *2020 global reassessment of the neutrino oscillation picture*, *JHEP* **02** (2021) 071 [[2006.11237](#)].
- [10] F. Capozzi, E. Di Valentino, E. Lisi, A. Marrone, A. Melchiorri and A. Palazzo, *The unfinished fabric of the three neutrino paradigm*, [2107.00532](#).
- [11] I. Esteban, M.C. Gonzalez-Garcia, M. Maltoni, T. Schwetz and A. Zhou, *The fate of hints: updated global analysis of three-flavor neutrino oscillations*, *JHEP* **09** (2020) 178 [[2007.14792](#)].
- [12] R. Mohapatra and J. Valle, *Neutrino Mass and Baryon Number Nonconservation in Superstring Models*, *Phys. Rev.* **D34** (1986) 1642.
- [13] J. Bernabeu, A. Santamaria, J. Vidal, A. Mendez and J.W.F. Valle, *Lepton Flavor Nonconservation at High-Energies in a Superstring Inspired Standard Model*, *Phys. Lett. B* **187** (1987) 303.
- [14] E.K. Akhmedov, M. Lindner, E. Schnapka and J. Valle, *Left-right symmetry breaking in NJL approach*, *Phys.Lett.* **B368** (1996) 270 [[hep-ph/9507275](#)].
- [15] E.K. Akhmedov, M. Lindner, E. Schnapka and J. Valle, *Dynamical left-right symmetry breaking*, *Phys.Rev.* **D53** (1996) 2752 [[hep-ph/9509255](#)].
- [16] R.N. Mohapatra and J.C. Pati, *Left-Right Gauge Symmetry and an Isoconjugate Model of CP Violation*, *Phys. Rev. D* **11** (1975) 566.
- [17] G. Senjanovic and R.N. Mohapatra, *Exact Left-Right Symmetry and Spontaneous Violation of Parity*, *Phys. Rev. D* **12** (1975) 1502.

- [18] I. Brivio and M. Trott, *The Standard Model as an Effective Field Theory*, *Phys. Rept.* **793** (2019) 1 [1706.08945].
- [19] J. Ellis, M. Madigan, K. Mimasu, V. Sanz and T. You, *Top, Higgs, Diboson and Electroweak Fit to the Standard Model Effective Field Theory*, *JHEP* **04** (2021) 279 [2012.02779].
- [20] J.J. Ethier, G. Magni, F. Maltoni, L. Mantani, E.R. Nocera, J. Rojo et al., *Combined SMEFT interpretation of Higgs, diboson, and top quark data from the LHC*, **2105.00006**.
- [21] F. del Aguila, S. Bar-Shalom, A. Soni and J. Wudka, *Heavy Majorana Neutrinos in the Effective Lagrangian Description: Application to Hadron Colliders*, *Phys. Lett. B* **670** (2009) 399 [0806.0876].
- [22] A. Aparici, K. Kim, A. Santamaria and J. Wudka, *Right-handed neutrino magnetic moments*, *Phys. Rev. D* **80** (2009) 013010 [0904.3244].
- [23] S. Bhattacharya and J. Wudka, *Dimension-seven operators in the standard model with right handed neutrinos*, *Phys. Rev. D* **94** (2016) 055022 [1505.05264].
- [24] Y. Liao and X.-D. Ma, *Operators up to Dimension Seven in Standard Model Effective Field Theory Extended with Sterile Neutrinos*, *Phys. Rev. D* **96** (2017) 015012 [1612.04527].
- [25] H.-L. Li, Z. Ren, M.-L. Xiao, J.-H. Yu and Y.-H. Zheng, *Operator Bases in Effective Field Theories with Sterile Neutrinos: $d \leq 9$* , **2105.09329**.
- [26] M. Chala and A. Titov, *One-loop matching in the SMEFT extended with a sterile neutrino*, *JHEP* **05** (2020) 139 [2001.07732].
- [27] M. Chala and A. Titov, *One-loop running of dimension-six Higgs-neutrino operators and implications of a large neutrino dipole moment*, *JHEP* **09** (2020) 188 [2006.14596].
- [28] A. Datta, J. Kumar, H. Liu and D. Marfatia, *Anomalous dimensions from gauge couplings in SMEFT with right-handed neutrinos*, *JHEP* **02** (2021) 015 [2010.12109].
- [29] A. Datta, J. Kumar, H. Liu and D. Marfatia, *Anomalous dimensions from Yukawa couplings in SMNEFT: four-fermion operators*, *JHEP* **05** (2021) 037 [2103.04441].
- [30] I. Bischer and W. Rodejohann, *General neutrino interactions from an effective field theory perspective*, *Nucl. Phys. B* **947** (2019) 114746 [1905.08699].
- [31] J. Alcaide, S. Banerjee, M. Chala and A. Titov, *Probes of the Standard Model effective field theory extended with a right-handed neutrino*, *JHEP* **08** (2019) 031 [1905.11375].
- [32] J.M. Butterworth, M. Chala, C. Englert, M. Spannowsky and A. Titov, *Higgs phenomenology as a probe of sterile neutrinos*, *Phys. Rev. D* **100** (2019) 115019 [1909.04665].
- [33] A. Biekötter, M. Chala and M. Spannowsky, *The effective field theory of low scale see-saw at colliders*, *Eur. Phys. J. C* **80** (2020) 743 [2007.00673].
- [34] W. Dekens, J. de Vries, K. Fuyuto, E. Mereghetti and G. Zhou, *Sterile neutrinos and neutrinoless double beta decay in effective field theory*, *JHEP* **06** (2020) 097 [2002.07182].
- [35] T. Han, J. Liao, H. Liu and D. Marfatia, *Scalar and tensor neutrino interactions*, *JHEP* **07** (2020) 207 [2004.13869].
- [36] T. Li, X.-D. Ma and M.A. Schmidt, *General neutrino interactions with sterile neutrinos in light of coherent neutrino-nucleus scattering and meson invisible decays*, *JHEP* **07** (2020) 152 [2005.01543].

- [37] T. Li, X.-D. Ma and M.A. Schmidt, *Constraints on the charged currents in general neutrino interactions with sterile neutrinos*, *JHEP* **10** (2020) 115 [[2007.15408](#)].
- [38] J. De Vries, H.K. Dreiner, J.Y. Günther, Z.S. Wang and G. Zhou, *Long-lived Sterile Neutrinos at the LHC in Effective Field Theory*, *JHEP* **03** (2021) 148 [[2010.07305](#)].
- [39] G. Cottin, J.C. Helo, M. Hirsch, A. Titov and Z.S. Wang, *Heavy neutral leptons in effective field theory and the high-luminosity LHC*, *JHEP* **09** (2021) 039 [[2105.13851](#)].
- [40] A. Caputo, P. Hernandez, J. Lopez-Pavon and J. Salvado, *The seesaw portal in testable models of neutrino masses*, *JHEP* **06** (2017) 112 [[1704.08721](#)].
- [41] D. Barducci, E. Bertuzzo, A. Caputo, P. Hernandez and B. Mele, *The see-saw portal at future Higgs Factories*, *JHEP* **03** (2021) 117 [[2011.04725](#)].
- [42] J.P. Chou, D. Curtin and H.J. Lubatti, *New Detectors to Explore the Lifetime Frontier*, *Phys. Lett. B* **767** (2017) 29 [[1606.06298](#)].
- [43] MATHUSLA collaboration, *An Update to the Letter of Intent for MATHUSLA: Search for Long-Lived Particles at the HL-LHC*, [2009.01693](#).
- [44] V.V. Gligorov, S. Knapen, M. Papucci and D.J. Robinson, *Searching for Long-lived Particles: A Compact Detector for Exotics at LHCb*, *Phys. Rev. D* **97** (2018) 015023 [[1708.09395](#)].
- [45] V.V. Gligorov, S. Knapen, B. Nachman, M. Papucci and D.J. Robinson, *Leveraging the ALICE/L3 cavern for long-lived particle searches*, *Phys. Rev. D* **99** (2019) 015023 [[1810.03636](#)].
- [46] J.L. Feng, I. Galon, F. Kling and S. Trojanowski, *ForwArd Search ExpeRiment at the LHC*, *Phys. Rev. D* **97** (2018) 035001 [[1708.09389](#)].
- [47] M. Bauer, O. Brandt, L. Lee and C. Ohm, *ANUBIS: Proposal to search for long-lived neutral particles in CERN service shafts*, [1909.13022](#).
- [48] J.C. Helo, M. Hirsch and Z.S. Wang, *Heavy neutral fermions at the high-luminosity LHC*, *JHEP* **07** (2018) 056 [[1803.02212](#)].
- [49] D. Dercks, H.K. Dreiner, M. Hirsch and Z.S. Wang, *Long-Lived Fermions at AL3X*, *Phys. Rev. D* **99** (2019) 055020 [[1811.01995](#)].
- [50] M. Hirsch and Z.S. Wang, *Heavy neutral leptons at ANUBIS*, *Phys. Rev. D* **101** (2020) 055034 [[2001.04750](#)].
- [51] G. Zhou, J.Y. Günther, Z.S. Wang, J. de Vries and H.K. Dreiner, *Long-lived Sterile Neutrinos at Belle II in Effective Field Theory*, [2111.04403](#).
- [52] G. Cottin, J.C. Helo and M. Hirsch, *Displaced vertices as probes of sterile neutrino mixing at the LHC*, *Phys. Rev. D* **98** (2018) 035012 [[1806.05191](#)].
- [53] S. Weinberg, *Baryon and Lepton Nonconserving Processes*, *Phys. Rev. Lett.* **43** (1979) 1566.
- [54] B. Grzadkowski, M. Iskrzynski, M. Misiak and J. Rosiek, *Dimension-Six Terms in the Standard Model Lagrangian*, *JHEP* **10** (2010) 085 [[1008.4884](#)].
- [55] N.D. Christensen and C. Duhr, *FeynRules - Feynman rules made easy*, *Comput. Phys. Commun.* **180** (2009) 1614 [[0806.4194](#)].

- [56] A. Alloul, N.D. Christensen, C. Degrande, C. Duhr and B. Fuks, *FeynRules 2.0 - A complete toolbox for tree-level phenomenology*, *Comput. Phys. Commun.* **185** (2014) 2250 [[1310.1921](#)].
- [57] C. Degrande, C. Duhr, B. Fuks, D. Grellscheid, O. Mattelaer and T. Reiter, *UFO - The Universal FeynRules Output*, *Comput. Phys. Commun.* **183** (2012) 1201 [[1108.2040](#)].
- [58] J. Alwall, M. Herquet, F. Maltoni, O. Mattelaer and T. Stelzer, *MadGraph 5 : Going Beyond*, *JHEP* **06** (2011) 128 [[1106.0522](#)].
- [59] J. Alwall, R. Frederix, S. Frixione, V. Hirschi, F. Maltoni, O. Mattelaer et al., *The automated computation of tree-level and next-to-leading order differential cross sections, and their matching to parton shower simulations*, *JHEP* **07** (2014) 079 [[1405.0301](#)].
- [60] ATLAS collaboration, *Search for massive, long-lived particles using multitrack displaced vertices or displaced lepton pairs in pp collisions at $\sqrt{s} = 8$ TeV with the ATLAS detector*, *Phys. Rev. D* **92** (2015) 072004 [[1504.05162](#)].
- [61] ATLAS collaboration, *Search for long-lived, massive particles in events with displaced vertices and missing transverse momentum in $\sqrt{s} = 13$ TeV pp collisions with the ATLAS detector*, *Phys. Rev. D* **97** (2018) 052012 [[1710.04901](#)].
- [62] T. Sjöstrand, S. Ask, J.R. Christiansen, R. Corke, N. Desai, P. Ilten et al., *An introduction to PYTHIA 8.2*, *Comput. Phys. Commun.* **191** (2015) 159 [[1410.3012](#)].
- [63] M. Cacciari, G.P. Salam and G. Soyez, *FastJet User Manual*, *Eur. Phys. J. C* **72** (2012) 1896 [[1111.6097](#)].
- [64] G. Cottin, J.C. Helo and M. Hirsch, *Searches for light sterile neutrinos with multitrack displaced vertices*, *Phys. Rev. D* **97** (2018) 055025 [[1801.02734](#)].
- [65] C. Degrande, O. Mattelaer, R. Ruiz and J. Turner, *Fully-Automated Precision Predictions for Heavy Neutrino Production Mechanisms at Hadron Colliders*, *Phys. Rev. D* **94** (2016) 053002 [[1602.06957](#)].
- [66] ATLAS collaboration, *Search for heavy neutral leptons in decays of W bosons produced in 13 TeV pp collisions using prompt and displaced signatures with the ATLAS detector*, *JHEP* **10** (2019) 265 [[1905.09787](#)].
- [67] CMS collaboration, *Search for heavy neutral leptons in events with three charged leptons in proton-proton collisions at $\sqrt{s} = 13$ TeV*, *Phys. Rev. Lett.* **120** (2018) 221801 [[1802.02965](#)].
- [68] CMS collaboration, *Search for long-lived heavy neutral leptons with displaced vertices in pp collisions at $\sqrt{s} = 13$ TeV with the CMS detector*, *CMS-PAS-EXO-20-009* (2021).
- [69] DELPHI collaboration, *Search for neutral heavy leptons produced in Z decays*, *Z. Phys. C* **74** (1997) 57.
- [70] LHCb collaboration, *Search for massive long-lived particles decaying semileptonically in the LHCb detector*, *Eur. Phys. J. C* **77** (2017) 224 [[1612.00945](#)].
- [71] S. Antusch, E. Cazzato and O. Fischer, *Sterile neutrino searches via displaced vertices at LHCb*, *Phys. Lett. B* **774** (2017) 114 [[1706.05990](#)].
- [72] M. Drewes and J. Hajer, *Heavy Neutrinos in displaced vertex searches at the LHC and HL-LHC*, *JHEP* **02** (2020) 070 [[1903.06100](#)].

- [73] S. Davidson, D.C. Bailey and B.A. Campbell, *Model independent constraints on leptoquarks from rare processes*, *Z. Phys. C* **61** (1994) 613 [[hep-ph/9309310](#)].
- [74] PARTICLE DATA GROUP collaboration, *Review of Particle Physics*, *Prog. Theor. Exp. Phys.* **2020** (2020) 083C01.
- [75] CMS collaboration, *Search for pair production of first-generation scalar leptoquarks at $\sqrt{s} = 13$ TeV*, *Phys. Rev. D* **99** (2019) 052002 [[1811.01197](#)].
- [76] CMS collaboration, *Search for dark matter in events with a leptoquark and missing transverse momentum in proton-proton collisions at 13 TeV*, *Phys. Lett. B* **795** (2019) 76 [[1811.10151](#)].
- [77] CMS collaboration, *Searches for physics beyond the standard model with the M_{T2} variable in hadronic final states with and without disappearing tracks in proton-proton collisions at $\sqrt{s} = 13$ TeV*, *Eur. Phys. J. C* **80** (2020) 3 [[1909.03460](#)].
- [78] ATLAS collaboration, *Search for scalar leptoquarks in pp collisions at $\sqrt{s} = 13$ TeV with the ATLAS experiment*, *New J. Phys.* **18** (2016) 093016 [[1605.06035](#)].
- [79] ATLAS collaboration, *Search for pairs of scalar leptoquarks decaying into quarks and electrons or muons in $\sqrt{s} = 13$ TeV pp collisions with the ATLAS detector*, *JHEP* **10** (2020) 112 [[2006.05872](#)].
- [80] CMS collaboration, *Search for long-lived particles that decay into final states containing two electrons or two muons in proton-proton collisions at $\sqrt{s} = 8$ TeV*, *Phys. Rev. D* **91** (2015) 052012 [[1411.6977](#)].
- [81] CMS collaboration, *Search for long-lived particles decaying to leptons with large impact parameter in proton-proton collisions at $\sqrt{s} = 13$ TeV*, [2110.04809](#).